

NANO IDEA

Open Access



# Highly Stretchable Micro/Nano Wrinkle Structures for Infrared Stealth Application

Jia Wang<sup>1,2</sup>, Yijun Li<sup>1</sup>, Jianli Cui<sup>2</sup> and Hao Guo<sup>2\*</sup> 

## Abstract

We demonstrate a novel infrared stealth structure consisting of  $\text{SiO}_2/\text{TiO}_2$  film, which was manufactured as the highly stretchable triangular wrinkle structures. The triangular wrinkle structures have firstly been transferred to the flexible substrate from the surface of Si-substrate, which was manufactured by the MEMS technology. Then, the infrared reflective film have been manufactured to be the triangular wrinkle structures by depositing the materials (noble metal (Ag or Au) or multilayer oxide ( $\text{SiO}_2/\text{TiO}_2$ )) on the surface of flexible substrate. Due to the lower reflection effect of curved surface, the infrared reflectivity of these structures has been tuned down to 5%. And, compared to the flat surface, the reflection-to-diffuse ratios improved approximately one order of magnitude. These structures can adapt to the environment by changing the reflectivity of triangular wrinkle structures under stretching. Finally, an Au-modified infrared stealth structure has been fabricated as the array structures, which disappeared and then display by stretching the triangular wrinkle structures at room temperature. It features high reflection-to-diffuse ratios, stable repeatability, low-cost, and easy to manufacture. It may open opportunities for infrared camouflage for military security and surveillance field application.

**Keywords:** Infrared stealth, Triangular wrinkle structures, Highly stretchable, Mechanical actuation

## Background

Infrared stealth technology has been widely used in field of spacecraft components [1], camouflage platforms [2], protective clothing [3], container packaging [4], and so on [5–7]. Especially to the military security and military surveillance field, which can protect the aircraft from detection.

In recent year, many materials, which statically reflect radiation in the infrared region of the electromagnetic spectrum, have been studied [8–10]. Wei et al. [11] proposed a metamaterial-based infrared reflection method by modulating the photo-generated carrier doping. Kocabas et al. [12] demonstrate active surfaces structures that can be controlled to tune the reflection, transmission, and absorption of microwaves. However, this kind of novel material was confined by complex technology, ultra-low production, and high cost.

To optimize the adaptabilities of infrared stealth structures, many different adaptive infrared materials

and structures have been designed and studied [13–15]. Valentine et al. [16] demonstrated a metamaterial-based infrared reflection method by spatiotemporally controlling the emissivity of metamaterial which is modulated with ultraviolet light. However, this structure has been actuated by the ultraviolet light, high temperatures, and large temperature gradients. Gorodetsky et al. [17] developed an adaptive infrared-reflecting structures based on the wrinkles structure with the feature of low working temperature, tuneable spectral range, fast response, and autonomous operation. However, this structure must be actuated by the high voltage about 3 kV, which is difficult to achieve in the common field, especially for aircraft.

In this study, a novel stretchable triangular wrinkle structure has been designed and manufactured to be the adaptive infrared stealth structure. The infrared reflectivity of this structure has been tuned to 5%, and a straightforward manufactured using the infrared reflecting materials was disappearance, and then display with the deformation of the triangular wrinkle structures under a simple mechanistically actuation at room temperature.

\* Correspondence: [guohao@nuc.edu.cn](mailto:guohao@nuc.edu.cn)

<sup>2</sup>Science and Technology on Electronic Test & Measurement Laboratory, North University of China, Taiyuan 030051, Shanxi, China  
Full list of author information is available at the end of the article

## Methods

The polydimethylsiloxane (PDMS) (10:1) membranes (Sylgard 184, Dow Corning) were prepared by spin coating on silicon wafers with a thickness of 500  $\mu\text{m}$  by controlling the spinning speed, and cured immediately after spinning at less than 80  $^{\circ}\text{C}$  for 2 h [18].

The silver film and the alternating layers of titanium dioxide ( $\text{TiO}_2$ ) and silicon dioxide ( $\text{SiO}_2$ ) were deposited on the PDMS substrates by the electron-beam evaporation according to the standard micro-fabrication techniques.

The total reflectance, diffuse reflectance, and total transmittance of our structures were characterized with a Frontier transform infrared spectrometer (Perkin Elmer). The measurements were performed at an illumination angle of 12 $^{\circ}$  over a wavelength range of 2 to 14  $\mu\text{m}$  and referenced to a diffuse gold standard (Pike Technologies).

The topography of the triangular wrinkle structure were characterized by laser scanning microscope (Model: LEXT OLS4100; Co.: Olympus) and atomic force microscope (AFM) (Model: Multimode8; Co.: Bruker). The infrared pictures and videos were obtained with a thermal imager camera (FOTRIC 226S) for the temperature and an effective spectral range from wavelengths of 8  $\mu\text{m}$  to 14  $\mu\text{m}$ .

## Results and Discussion

### Infrared Stealth Mechanism

Schematics of the infrared reflecting structures were depicted in Fig. 1. We investigated the properties of infrared reflectance based on the triangular structure. The model of infrared stealth was simulated by the software of Zemax. As the light was incident on a flat structure, the most the incident light would reflected along a determined direction following the law of reflection, as shown in Fig. 1a. When the light was incident on the triangular structures, most of the light fall inside the triangular trap structures and only a litter light can reflect out of the triangular structures, as depicted in Fig. 1b. That is, as the infrared light was incident into the triangular structure, most of the

infrared light would not be detected using the reflection mechanism of light. This triangular structure can be invisible for the infrared detection technique.

### Fabrication of Triangular Wrinkle Structure

As shown in Fig. 2, the triangular wrinkle structures were fabricated using the MEMS technology, which have been reported in our previous work [19]. First, a positive photoresist was spin-coated on the silica wafer at 3000 rad/min and baked at 105  $^{\circ}\text{C}$  for 90 s. Second, the wafer was exposed to a dose of 135  $\text{mJ}/\text{cm}^2$  with a mask aligner and baked at 115  $^{\circ}\text{C}$  for 120 s to form strong crosslinks. After the wafer had gradually cooled down, the structure was immersed in a positive developer (40 s). Third, etch  $\text{SiO}_2$  using a buffered oxide etch and etch Si using 15 wt% TMAH + 17 vol% isopropyl alcohol (22 min). Fourth, a  $\text{SiO}_2$  layer was removed by the hydrofluoric acid. Then, a triangular-like structure was obtained, as shown in Fig. 2a [6]. Fifth, a PDMS mold was prepared by mixing the liquid PDMS elastomer and curing agent at a 10:1 ratio in volume, which was poured onto the Si mold and was thermally cured at 80  $^{\circ}\text{C}$  for 1.5 h to obtain the triangular structure on the surface of PDMS substrate to form the PDMS mold. Then, a  $\text{SiO}_x$  layer and hydrophilic groups (e.g., -OH) have been formed on the surface of the PDMS substrate under oxygen plasma treatment at 150 W for 15 s. The sample was then immersed in an SDS solution for 15 s to introduce  $-\text{SO}_3^-$  groups at the surface of the triangular wrinkled PDMS structure. This process can introduce a condensation reaction of hydrophilic functionalities between the PDMS and noble metal (Ag, Au) and oxide materials ( $\text{SiO}_2$ ,  $\text{TiO}_2$ ), which have been reported in detail in our previous work [20–22]. Finally, metal or oxide triangular wrinkle structure were obtained by coating the metal or oxide on the surface of the PDMS mold using the electron-beam evaporation technology, which have been reported in detail in our previous work [20–22].

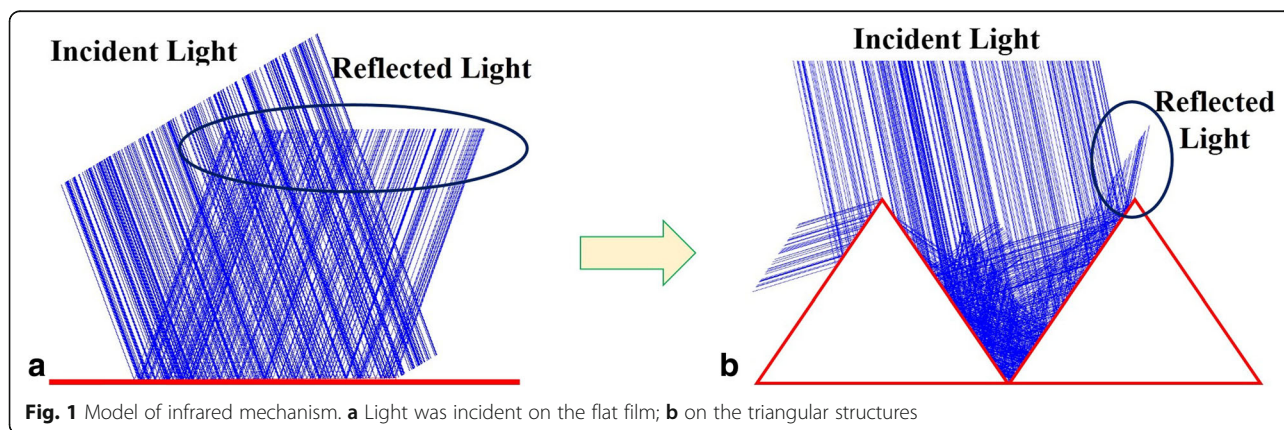
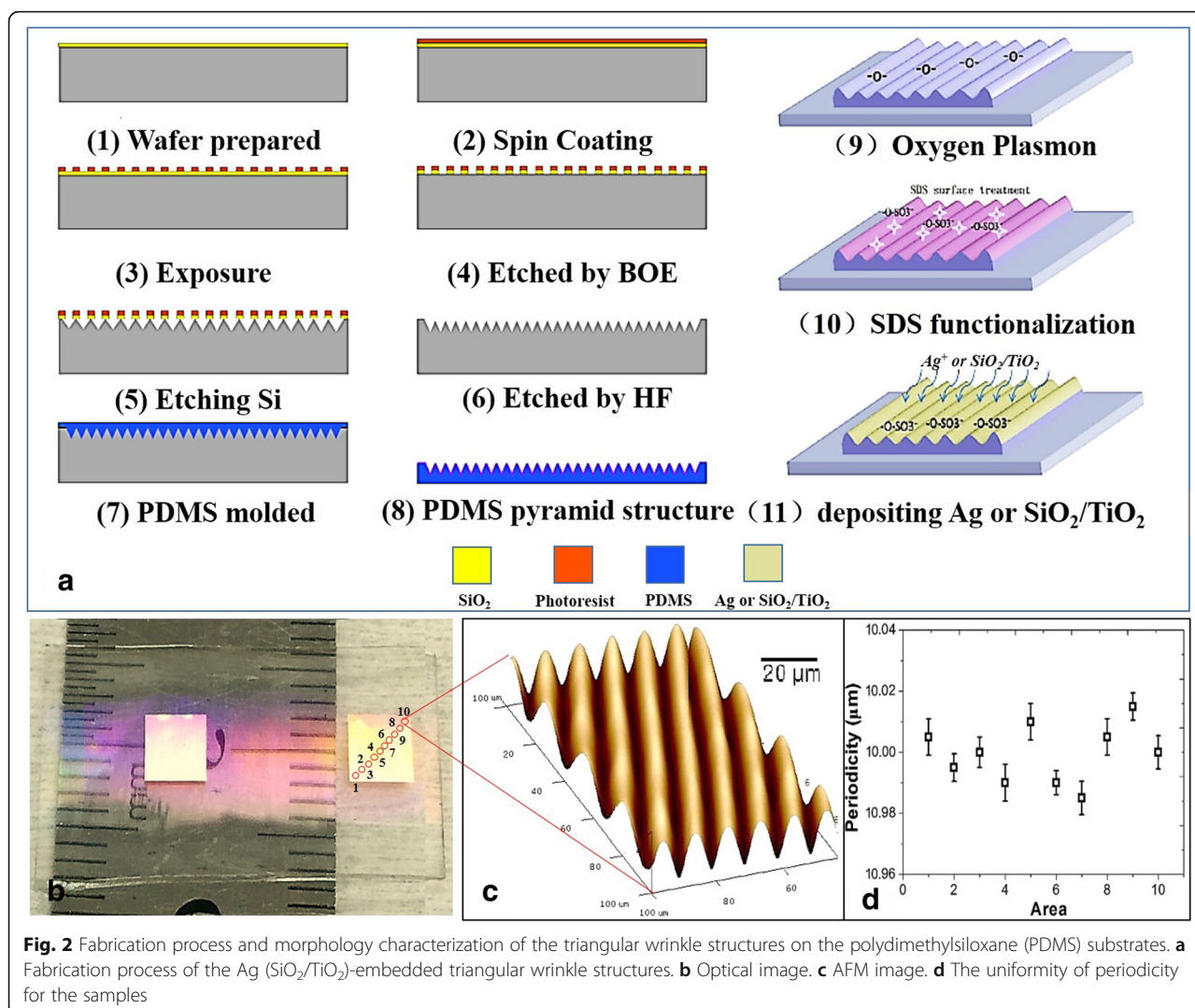


**Fig. 1** Model of infrared mechanism. **a** Light was incident on the flat film; **b** on the triangular structures



As shown in Fig. 2b–d, the periodicity of triangular wrinkle structures was uniform, and the periodicity was about  $(10 \pm 0.1) \mu\text{m}$  on the whole surface of the sample tested by atomic force microscopy. And the size of sample was about  $4 \text{ mm} \times 4 \text{ mm}$ . Desired periodicity was achieved by tuning the size of mask structures and etch parameters, which can be calculated as introduced in our previous studies [19].

### Infrared Stealth Testing

In our work, the metal triangular wrinkle structures have been firstly fabricated to investigate the infrared reflection effect. Due to the high ductility, excellent bendability, and relatively low hardness and cost, metal Ag materials have been selected to manufacture the infrared reflective film. The Ag triangular wrinkle structures have been fabricated following the process of Fig. 2a.

Before mechanical actuation, when a beam of light is incident on the tip of the triangular infrared reflective structure (Fig. 3a), most of the infrared ray (red line) has been diffused by the tip (blue line) and only a little light can be reflected (green line) into the detector. While after mechanical actuation, the surface of triangular structure can be gradually stretched to be plane as shown in Fig. 3b. In the case, most of the incident light would reflect into the detector.

The corresponding infrared spectra have proved the above results in our experiment as shown in Fig. 3c. As unactuated triangular wrinkle structures, it featured a high average total reflectance of  $46 \pm 2\%$ , a low average reflection of  $< 13\%$ , and a moderate average diffuse light of  $33 \pm 2\%$ . Hence, the total reflectance featured a weak average reflection of  $13 \pm 2\%$  and a dominant average diffuse component of  $33 \pm 2\%$ , in a ratio of  $\sim 0.4$ . After mechanically stretching the triangular wrinkle structures

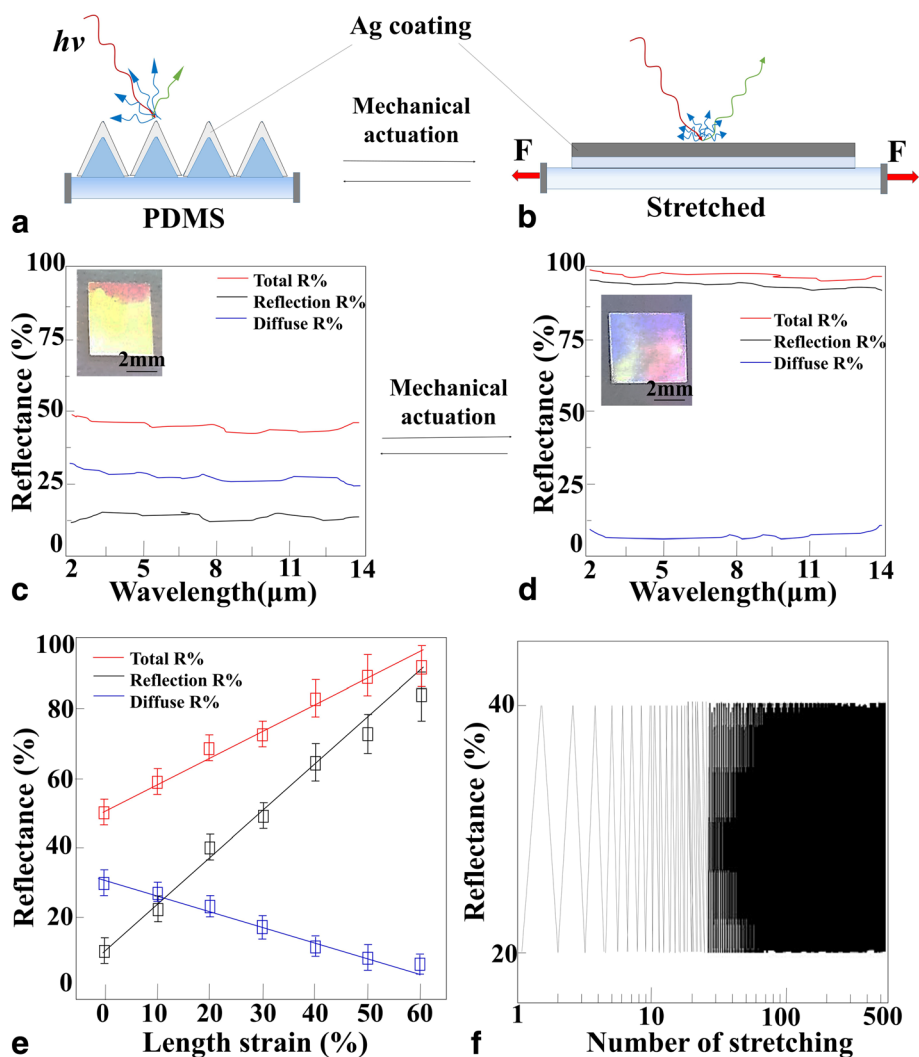


**Fig. 3** Mechanical modulation of the broadband reflectance. **a** The change in the surface morphology and the reflection of infrared light of the Ag triangular wrinkle structures before mechanical actuation. **b** After mechanical actuation. **c** The infrared reflectance spectra of the Ag triangular wrinkle structures before mechanical actuation. The total reflectance (red traces) are shown along with their reflection (black traces) and diffuse (blue traces) components. **d** After mechanical actuation. **e** Plots of the total, reflection, and diffuse peak reflectance of the Ag triangular wrinkle structures as functions of the applied length strain. **f** Stability test of the Ag triangular wrinkle structures with stretching/releasing over 500 cycles

(as shown in Fig. 3d), the corresponding infrared spectra featured an increased average total reflectance of  $97 \pm 1\%$ , a high average reflection of  $89 \pm 1\%$ , and a low average total diffuse light of  $8 \pm 1\%$ .

From the experiment results, the reflectivity increased from 13 to 89% with stretching the triangular Ag wrinkle structures. Also, the diffuse light has been reduced from 33 to 8%. The reason was that the triangular Ag wrinkle structures have been stretched to be Ag plane film. The incident light can reflect along a certain angle from the plane film following the law of reflection. Due to the high reflectivity of plane film, the total reflectance can be up to 100% in theory and the diffuse light was only a small amount. Considering the rough surface of Ag film, the

reflection would be reduced (89%) and the diffused light would be increased (8%).

Meanwhile, compared to the wrinkle structure, the diffused light reduced from 33 to 8% from the plane film. The reason was that the roughness of the triangular Ag wrinkle structures was about  $\sim 1 \mu\text{m}$  depended by the height of wrinkle structures. But for the Ag plane film, the roughness was about  $\sim 20 \text{ nm}$  or smaller, which was the roughness of Ag film. Hence, the diffuse light can be further reduced by optimizing the technological parameter of electron-beam evaporation.

In this case, the total reflectance featured a much larger average reflection of  $89 \pm 1\%$  and a smaller average diffuse light component of  $8 \pm 1\%$ , in a ratio of  $\sim 11$ . Hence, the



reflection-to-diffuse ratios have been approximately increased an order of magnitude based on triangular wrinkle structures.

In general, the total reflectance of triangular wrinkle structures at broadband wavelength increased as a function of the strain (Fig. 3e). The reflectivity increased with the strain, but the diffuse reduced, as stretching the triangular wrinkle Ag film to be flat. The infrared reflection properties were fully reversible on repeated mechanical actuation contributing to the highly stretchable property of wrinkle structures. And only minor performance degradation has been observed after 500 cycles (Fig. 3f). Thus, mechanical actuation of our triangular wrinkle structures induced a change, which can be reversible and dynamically modulated of the broadband reflectance within the short- to long-wavelength infrared region.

In general, compare to the broadband infrared technology, the narrow infrared band has the higher signal-to-noise ratio and easier traceability for infrared target detection, discernment, and tracking application.

Hence, to improve the precision of infrared target detection, discernment, and tracking technology, the narrowband

infrared reflection effect of triangular wrinkle structures has been investigated as shown in Fig. 4.

To obtain narrowband infrared reflectance peak, alternating  $\text{TiO}_2/\text{SiO}_2/\text{TiO}_2/\text{SiO}_2/\text{TiO}_2$  layers with thicknesses of  $\lambda_{\text{peak}}/(4 \times n_{\text{TiO}_2})$  and  $\lambda_{\text{peak}}/(4 \times n_{\text{SiO}_2})$  have been designed. The structures were manufactured according to standard lithographic protocols as shown in Fig. 2a. The  $\text{TiO}_2/\text{SiO}_2$  Bragg stacks with a peak reflectance intensity at  $5 \mu\text{m}$  was produced with the  $\text{SiO}_2$  thickness was  $0.933 \mu\text{m}$  and the  $\text{TiO}_2$  thickness was  $0.543 \mu\text{m}$  by an Angstrom Engineering EvoVac system. The narrowband infrared reflection structures consist of two-layer  $\text{SiO}_2$  and three-layer  $\text{TiO}_2$ . And the size of narrowband infrared reflection structures based on the triangular wrinkle structures was about  $4 \text{ mm} \times 4 \text{ mm}$ .

In our works, before mechanical actuation, the narrowband infrared reflection structures based on the triangular wrinkle structures, the infrared spectra featured the total reflectance intensities of  $18 \pm 2\%$  at a wavelength of  $5 \mu\text{m}$ , with a weak average reflection of  $5 \pm 2\%$  and an average diffuse component of  $13 \pm 2\%$ , in a ratio of  $\sim 0.38$ , as shown in Fig. 4c.

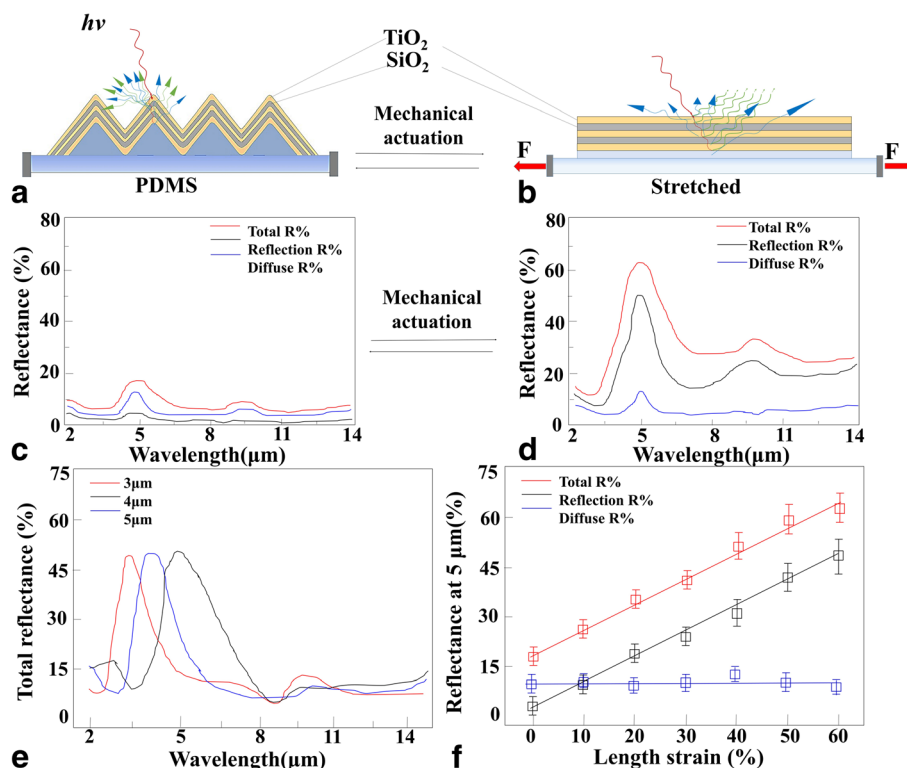


**Fig. 4** Mechanical modulation of the narrowband reflectance. **a** The change in the surface morphology and the reflection of infrared light of a  $\text{TiO}_2/\text{SiO}_2$  Bragg stack-modified structures before mechanical actuation. **b** After mechanical actuation. **c** The infrared reflectance spectra of a  $\text{TiO}_2/\text{SiO}_2$  Bragg stack-modified structures with a peak reflectance intensity at  $5 \mu\text{m}$  before mechanical actuation. The total reflectance (red traces) are shown along with their reflection (black traces) and diffuse (blue traces) components. **d** After mechanical actuation. **e** The infrared spectra of three unactuated devices that have been designed to feature peak reflectance wavelengths of  $3 \mu\text{m}$  (red trace),  $4 \mu\text{m}$  (blue trace), and  $5 \mu\text{m}$  (black trace). **f** Plots of the total, reflection, and diffuse peak reflectance of the  $\text{TiO}_2/\text{SiO}_2$  Bragg stack-modified structures as functions of the applied length strain

After mechanical actuation, the total reflectance intensities increased up to  $63 \pm 4\%$  at a wavelength of  $5 \mu\text{m}$ , with a much larger reflection component of  $50 \pm 3\%$  and a nearly unchanged diffuse component of  $13 \pm 2\%$  in a ratio of  $\sim 3.8$  (as shown in Fig. 4d). This result was consistent with the Ag-modified reflective film based on the triangular wrinkle structures. The reflectivity increased from 5 to 63% caused by the reasons that the triangular  $\text{TiO}_2/\text{SiO}_2$  multi-layers wrinkle structures have been stretched to be plane film. The incident infrared light can reflect along a certain angle from the plane film to improve the reflectivity.

Similarly, for narrowband infrared reflectivity structure based on the triangular wrinkle structures, the reflection-to-diffuse ratios reduced about one order of magnitude at a wavelength of  $5 \mu\text{m}$ . Also, the same results can be proved at the wavelengths of 3, 4, and  $5 \mu\text{m}$  (owing to the change of thickness of the  $\text{TiO}_2$  and  $\text{SiO}_2$ ), as shown in Fig. 4e.

In general, the total reflectance of triangular wrinkle structures at broadband wavelength increased as a function of the strain (Fig. 4f). The reflection increased with the strain, but the diffuse components remained relatively unaffected. The reason was that the roughness of the triangular wrinkle structures and the plane film was about the same size. The height of wrinkle structures was reduced from  $\sim 1 \mu\text{m}$  to  $\sim 200 \text{ nm}$  with covering the  $\text{TiO}_2$  or  $\text{SiO}_2$  film. Because the corner between two triangular structures would cover more film than other area, which would reduce the height of  $\text{TiO}_2/\text{SiO}_2$  multi-layers film wrinkle structures. The

more the thickness of film increased, the more the height reduced. While for the  $\text{TiO}_2/\text{SiO}_2$  plane film, the roughness was about  $\sim 50 \text{ nm}$  caused by the worse quality for the oxide than the metal using the MEMS technology.

### Demonstration of Application Examples

As a proof-of-concept for infrared stealth of triangular wrinkle structures, we evaluated our infrared stealth structures to conceal themselves under infrared visualization.

We designed and manufactured an Au-modified infrared reflective film with three-by-three arrays structures. The size of the sample was  $5 \text{ cm} \times 5 \text{ cm}$  and imaged by a thermal infrared camera, as shown in Fig. 5a. The three-by-three arrays structures served as the label composed of PDMS-nanodiamond composite materials, which have high infrared transmission materials, as shown in Fig. 5b.

Before mechanical actuation, the triangular Au-modified wrinkle structures were clearly observed by the laser scanning confocal microscopy as shown in the inset in Fig. 5c (left). From the sectional view of inset, triangular structure can be seen clearly. And the corresponding infrared image can be shown in Fig. 5d (left). Without actuation, there was only an overall outline of Au-modified film structures. As the strain increased from 0 to 60%, the triangular wrinkle structure had been stretched to become flat and the height decreased to zero, which was observed by the laser scanning confocal microscopy. And the corresponding infrared image have shown that the Au-modified film structures gradually become red caused by the increased

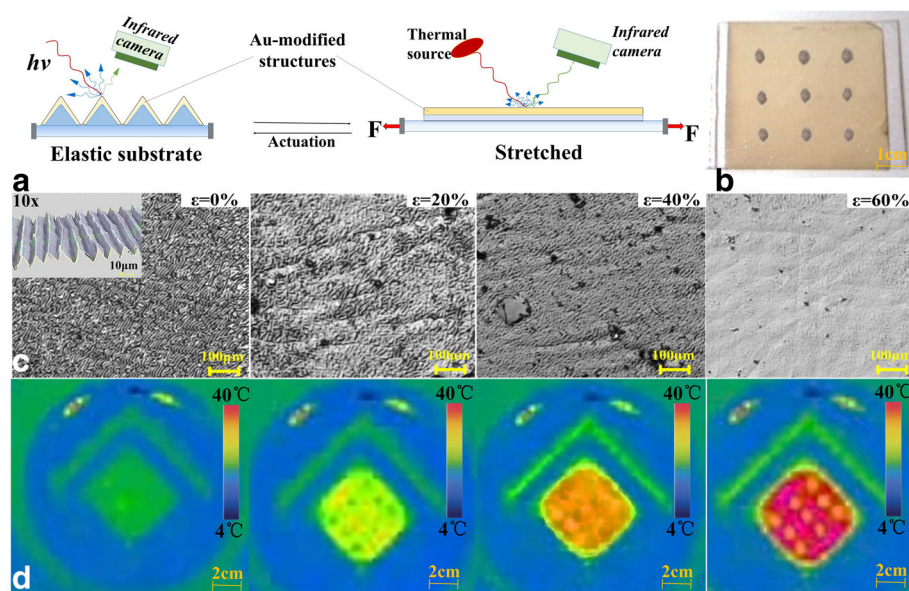


**Fig. 5** Reversible stealth of Au-modified structures in the infrared. **a** Schematics of an Au-modified structures under a constant thermal flux (left) before and (right) after mechanical actuation. **b** Optical image of Au-modified structures. **c** The microscopic morphological characteristics for triangular wrinkle structures with increasing the strain. **d** The corresponding infrared camera images of the same Au-modified structures with increasing the strain

infrared reflectivity. And the three-by-three arrays structure was emerging to be a hole. Hence, the results prove the infrared stealth effect of the triangular wrinkle structures with the advantage of repeatability, stability, and fully reversibility.

## Conclusions

We have examined the infrared stealth properties of noble metal (Au and Ag) and metal oxide ( $\text{TiO}_2/\text{SiO}_2$ )-modified stretchable triangular wrinkle structures.

First, the infrared reflectivity of these structures has been tuned from 50 to 5% and the reflection-to-diffuse ratios dynamically modulated by approximately order of magnitude. Second, our presented structures feature capabilities for adaptive infrared camouflage technologies at the broadband and narrowband wavelength. Third, the structures have been straightforward integrated and featured stability to repeated cycling. Last, the structures enable new autonomous portable technologies under a simple mechanically actuation at room temperature. Ultimately, the described structures may afford new possibilities for infrared camouflage applied in the field of military security and surveillance.

## Abbreviations

AFM: Atomic force microscope; PDMS: Polydimethylsiloxane

## Funding

This work was financially supported by the China Postdoctoral Innovative Talents Support Program (BX20180276), the National Natural Science Foundation of China (51635011 and 51727808), and the Shanxi "1331 Project" Key Subjects Construction.

## Availability of Data and Materials

They are all in the main text and figures.

## Authors' Contributions

JW performed the measurements and wrote the main manuscript text. HG conceived the idea. JC prepared the samples. JL modified the manuscript. All authors contribute the analysis and discussion of the experimental data and approved the final manuscript.

## Competing Interests

The authors declare that they have no competing interests.

## Publisher's Note

Springer Nature remains neutral with regard to jurisdictional claims in published maps and institutional affiliations.

## Author details

<sup>1</sup>Department of Physics, School of science, North University of China, Taiyuan 030051, Shanxi, China. <sup>2</sup>Science and Technology on Electronic Test & Measurement Laboratory, North University of China, Taiyuan 030051, Shanxi, China.

Received: 24 July 2018 Accepted: 31 October 2018

Published online: 13 November 2018

## References

- Dai GL, Shang J, Huang JP (2018) *Phys Rev E* 97(2):022129
- Li Y, Shen XY, Wu ZH, Huang JY, Chen YX, Ni YS, Huang JP (2015) *Phys Rev Lett* 115(19):195503
- Xu HY, Shi XH, Gao F, Sun HD, Zhang BL (2014) *Phys Rev Lett* 112(5):054301
- Yang TZ, Wu QH, Xu WK, Liu D, Huang LJ, Chen F (2016) *Phys Rev A* 380(7–8):965–969
- El-Ganainy R, Makris K, Khajavikhan M, Musslimani Z, Rotter S, Christodoulides D (2018) *Nat Phys* 14:11–19
- Zigoneanu L, Popa B, Cummer S (2014) *Nat Mater* 13(4):352–355
- Han TC, Bai X, Gao DL, Thong JTL, Li BW, Qiu CW (2014) *Phys Rev Lett* 112(5):054302
- Niu S, Joe G, Zhao H, Zhou Y, Orvis T, Huyen H, Salman J, Mahalingam K, Urwin B, Wu J, Liu Y, Tiwald T, Cronin S, Howe B, Mecklenburg M, Haiges R, Singh D, Wang H, Kats M, Ravichandran J (2018) *Nat Photonics* 12:392–396
- Arbabi A, Arbabi E, Horie Y, Kamali SM, Faraon A (2017) *Nat Photonics* 11(7):415
- Giddens H, Yang L, Tian J, Hao Y (2018) *IEEE Photon Technol Lett* 30(8):748–751
- Xiao L, Ma H, Liu J, Zhao W, Jia Y, Zhao Q, Liu K, Wu Y, Wei Y, Fan S, Jiang K (2015) *Nano Lett* 15:8365–8370
- Balci O, Polat E, Kakenov N, Kocabas C (2015) *Nat Commun* 6:6628
- Maldovan M (2013) *Nature* 503:209–217
- Li Y, Bai X, Yang T, Luo H, Qiu C (2018) *Nat Commun* 9:273
- Liu D, Cheng H, Xing X, Zhang C, Zheng W (2016) *Infrared Physics and Technology* 77:339–343
- Coppens Z, Valentine J (2017) *Adv Mater* 29:1701275
- Xu C, Stiubianu G, Gorodetsky A (2018) *Science* 359:1495–1500
- Duan J, Zhu Q, Qian K, Guo H, Zhang B (2017) *Nanoscale Res Lett* 12:515
- Cui J, Zhang B, Duan J, Guo H, Tang J (2017) *Materials* 10(12):1439
- Tang J, Guo H, Zhao M, Yang J, Tsoukalas D, Zhang B, Liu J, Xue C, Zhang W (2015) *Sci Rep* 5:16527
- Guo H, Tang J, Zhao M, Zhang W, Yang J, Zhang B, Chou X, Liu J, Xue C, Zhang W (2016) *Nanoscale Res Lett* 11:112
- Tang J, Guo H, Chen M, Yang J, Tsoukalas D, Zhang B, Liu J, Xue C, Zhang W (2015) *Sens Actuators B Chem* 218:145–151

**Submit your manuscript to a SpringerOpen<sup>®</sup> journal and benefit from:**

- Convenient online submission
- Rigorous peer review
- Open access: articles freely available online
- High visibility within the field
- Retaining the copyright to your article

Submit your next manuscript at ► [springeropen.com](https://www.springeropen.com)